



# Leaf waxes in litter and topsoils along a European transect

Imke K. Schäfer<sup>1</sup>, Verena Lanny<sup>2</sup>, Jörg Franke<sup>1</sup>, Timothy I. Eglinton<sup>2</sup>, Michael Zech<sup>3,4</sup>,  
Barbora Vysloužilová<sup>5,6</sup>, and Roland Zech<sup>1</sup>

<sup>1</sup>Institute of Geography and Oeschger Centre for Climate Change Research, University of Bern,  
3012 Bern, Switzerland

<sup>2</sup>Department of Earth Science, ETH Zurich, 8092 Zurich, Switzerland

<sup>3</sup>Landscape- & Geoecology, Faculty of Environmental Sciences, Technical University of Dresden,  
01062 Dresden, Germany

<sup>4</sup>Institute of Agronomy and Nutritional Sciences, Soil Biogeochemistry, Martin Luther University  
Halle-Wittenberg, 06120 Halle, Germany

<sup>5</sup>Institute of Archaeology of Academy of Science of the Czech Republic, Letenská 4,  
11801 Prague 1, Czech Republic

<sup>6</sup>Laboratoire Image, Ville, Environnement, UMR7362, CNRS/Université de Strasbourg,  
67083 Strasbourg CEDEX, France

*Correspondence to:* Imke K. Schäfer (imke.schaefer@giub.unibe.ch)

Received: 20 May 2016 – Published in SOIL Discuss.: 30 May 2016

Revised: 10 October 2016 – Accepted: 13 October 2016 – Published: 25 October 2016

**Abstract.** Lipid biomarkers are increasingly used to reconstruct past environmental and climate conditions. Leaf-wax-derived long-chain *n*-alkanes and *n*-alkanoic acids may have great potential for reconstructing past changes in vegetation, but the factors that affect the leaf wax distribution in fresh plant material, as well as in soils and sediments, are not yet fully understood and need further research. We systematically investigated the influence of vegetation and soil depth on leaf waxes in litter and topsoils along a European transect. The deciduous forest sites are often dominated by the *n*-C<sub>27</sub> alkane and *n*-C<sub>28</sub> alkanolic acid. Conifers produce few *n*-alkanes but show high abundances of the C<sub>24</sub> *n*-alkanoic acid. Grasslands are characterized by relatively high amounts of C<sub>31</sub> and C<sub>33</sub> *n*-alkanes and C<sub>32</sub> and C<sub>34</sub> *n*-alkanoic acids. Chain length ratios thus may allow for distinguishing between different vegetation types, but caution must be exercised given the large species-specific variability in chain length patterns. An updated endmember model with the new *n*-alkane ratio  $(n\text{-C}_{31} + n\text{-C}_{33}) / (n\text{-C}_{27} + n\text{-C}_{31} + n\text{-C}_{33})$  is provided to illustrate, and tentatively account for, degradation effects on *n*-alkanes.

## 1 Introduction

To improve our understanding of ongoing environmental changes and to predict consequences of future climate change more precisely, it is important to investigate the magnitude of, and interactions between, climate and environmental variations in the past. Lipid biomarkers are well preserved in many geological archives and are increasingly used for palaeoclimate and palaeoenvironmental reconstructions (Eglinton and Eglinton, 2008). Long-chain *n*-alkanes

(> C<sub>25</sub>) and *n*-alkanoic acids (> C<sub>20</sub>), for example, are essential constituents of epicuticular leaf waxes and thus serve as specific biomarkers for higher terrestrial plants (Eglinton et al., 1962; Eglinton and Hamilton, 1967; Otto and Simpson, 2005).

Leaf wax *n*-alkanes typically show an odd-over-even predominance (OEP; Eglinton and Hamilton, 1967). The relative odd homologue abundance may be useful to discriminate between different vegetation types: C<sub>27</sub> and C<sub>29</sub> have been reported to be predominant in leaf waxes of trees and shrubs,

whereas  $C_{31}$  and  $C_{33}$  mostly derive from grasses and herbs (Maffei, 1996; Maffei et al., 2004; Rommerskirchen et al., 2006; Zech et al., 2009; Lei et al., 2010; Kirkels et al., 2013). From this distribution, various  $n$ -alkane ratios have been proposed that allow estimating the main contributing vegetation type to a palaeosample (Schwark et al., 2002; Zech et al., 2009; Lei et al., 2010; Schatz et al., 2011; Wiesenberg et al., 2015). Where pollen grains are preserved, leaf wax and pollen records are in good agreement (e.g. Brincat et al., 2000; Schwark et al., 2002; Zech et al., 2010; Tarasov et al., 2013). In contrast, a recent study that summarizes  $n$ -alkane patterns in modern plants from all over the world showed no discrimination power for vegetation reconstruction at a global scale (Bush and McInerney, 2013), so regional calibration studies may be more appropriate. Additionally, the accuracy of  $n$ -alkane records remains somewhat uncertain due to several potential pitfalls:

- i. Leaf wax production and concentration can vary widely between species (e.g. Diefendorf et al., 2011; Bush and McInerney, 2013). Moreover, species abundance in an ecosystem controls leaf wax signals in soils and sediment.
- ii. Several studies reported long-chain  $n$ -alkanes not only in leaves but also in other plant parts (roots, stems, blossoms; e.g. Wöstmann, 2006; Jansen et al., 2006; Kirkels et al., 2013; Gocke et al., 2013), but in these studies the patterns show preferential synthesis of shorter chains ( $< n-C_{25}$ ) with low OEPs, as well as much lower  $n$ -alkane concentrations (3 to 10 times) than in leaves.
- iii. Leaf waxes are affected by mineralization and degradation (e.g. Zech et al., 2009, 2011a; Nguyen Tu et al., 2011). As OEP values become lower during degradation, Zech et al. (2009) and Buggle et al. (2010) proposed procedures to quantify and correct  $n$ -alkane ratios for degradation using the OEP.
- iv. Apart from vegetation type, many environmental parameters may influence leaf wax patterns, for example temperature and precipitation (e.g. Poynter et al., 1989; Sachse et al., 2006; Tipple and Pagani, 2013; Bush and McInerney, 2015), as well as radiation, nutrient and water availability, salinity, mechanical stress and pollution (e.g. Shepherd and Wynne Griffiths, 2006; Guo et al., 2014). Sachse et al. (2006) and Duan and He (2011) found longer chain lengths at lower latitudes, which could indicate (i) enhanced loss of shorter  $n$ -alkanes with increasing evaporation and (ii) preferential production of long-chain  $n$ -alkanes, providing better protection against evaporation at higher temperatures and radiation. Schefuß et al. (2003) reported a higher  $n-C_{31}$  vs.  $n-C_{29}$  abundance in dust samples from drier regions along the West African margin and suggested that humidity may be the driving factor. Bush and McInerney (2015) showed a correlation between average chain

length (ACL) and temperature along a transect throughout the central United States and concluded that temperature is directly responsible for the synthesis of longer chain length.

So far, only few studies have investigated homologue long-chain  $n$ -alkanoic acid patterns in plants, soils and sediments (e.g. Almendros et al., 1996; Marseille et al., 1999; Bull et al., 2000b; Zocatelli et al., 2012; Feakins et al., 2014; Wiesenberg et al., 2015). Leaf wax  $n$ -alkanoic acids have a distinct even-over-odd predominance (EOP; Eglinton and Hamilton, 1967). Zocatelli et al. (2012) found  $n-C_{26}$  to be predominant in grassland soil relative to forest soil, whereas the forest soils contained  $n-C_{22}$  to  $n-C_{28}$  in greater amounts. Since  $n$ -alkane patterns alone seem to not always allow a reliable conclusion about the dominant vegetation type, there is an urgent need to more systematically investigate and understand the factors controlling the homologue  $n$ -alkanoic acid patterns.

In order to contribute to a better understanding of the various factors controlling leaf wax patterns, we collected and analysed litter and topsoil samples in deciduous and coniferous forests and from grasslands along a transect in central Europe.

Specifically, our study aims to evaluate (1) the role of different vegetation types for  $n$ -alkane and  $n$ -alkanoic acid chain length patterns and (2) the effects of degradation on leaf wax patterns.

Sampling of litter and topsoil samples rather than individual plants or plant parts has the advantage of integrating over the whole ecosystem and implicitly taking into account variable production and concentration of leaf waxes between species, individual plants and plant parts. Such an approach also implicitly accounts for the fact that vegetation types generally do not totally dominate a specific ecosystem but mostly co-occur to a variable degree. For example, we defined forests with a dominance  $> 80\%$  of deciduous or coniferous trees as deciduous or coniferous forests, respectively, and forests generally have some grass and herb understorey as well. Our study will thus provide leaf wax patterns for ecosystems dominated by specific vegetation types, and those patterns will be a sound basis for comparing and interpreting leaf wax patterns from palaeosols or sediments. Changes in leaf wax patterns from litter to the topsoil are expected to indicate effects of degradation and microbial reworking of organic material in the topsoil. Differences in climatic conditions along the transect are not very pronounced, so this paper cannot focus on potential direct climatic effects on leaf wax patterns.

## 2 Material and methods

### 2.1 Geographical setting and sampling

In 2012 and 2014, we collected litter (L) and topsoil samples (Ah1: 0–3 cm; Ah2: 3–10 cm) from 26 locations along a tran-

sect in central Europe (Fig. 1). Samples BRO, HUB, HUG, HUM, HUR and KOC were kindly provided by B. Vysloužilová; more information about sampling and the regional setting of these locations can be found in Vysloužilová et al. (2015). The study area is in general characterized by relatively mild temperatures and moderate rainfall. The mean annual air temperature along the transect ranges from 5.5 to 11.0 °C, and mean annual precipitation ranges from 470 to 1700 mm (see Table S1 in the Supplement for individual data and data source). Altitudes range from 16 to 899 m a.s.l. (above sea level). The natural vegetation consists of grasslands in the south of the transect and a higher amount of deciduous broadleaf and mixed forests (varying percentages of deciduous trees and conifers) in the north. Also, the proportion of evergreen conifers increases northwards.

We sampled soils in forests with a dominance of deciduous and coniferous trees, as well as soils below grasslands (referred to as “dec”, “con” and “grass” in the following text and figures). Photographs of the sampling sites and descriptions of the dominant vegetation are provided in Tables S2 and S1, respectively. For the dec and con sites, we were able to collect litter samples, but the grass sites had virtually no litter. Sampling sites were chosen in forests with large old trees, indicating a stable environment for more than approximately 30 years. This limits the risk that a vegetation change might have influenced the leaf wax signal in the soil, as leaf waxes are stable over long time periods (e.g. Derenne and Largeau, 2001). Please note that our grass sites can be dominated by grasses, herbs or heaths. Soil and litter samples at each site were composites from three sampling points approximately 5 to 7 m apart from each other.

## 2.2 Lipid analysis

Lipids were extracted from 1–6 g freeze-dried and ground samples by microwave extraction with 15 mL of dichloromethane (DCM)/methanol (MeOH) (9:1) at 100 °C for 1 h. Each total lipid extract was passed over a pipette column filled with aminopropyl silica gel as the stationary phase (Supelco, 45 µm). The apolar fraction (including *n*-alkanes) was eluted with hexane, more polar compounds (e.g. alcohols) with DCM/MeOH (1:1), and acids (including *n*-alkanoic acids) with 5% acetic acid in diethyl ether. The *n*-alkanes were purified by passing the apolar fraction over a pipette column filled with activated AgNO<sub>3</sub> impregnated silica gel (to retain unsaturated compounds) and another pipette column filled with zeolite (Geokleen). After drying, the zeolite (containing straight-chain compounds) was dissolved in HF and the *n*-alkanes were recovered by liquid–liquid extraction with hexane. For quantification, the *n*-alkane fractions were spiked with a known amount of the 5 $\alpha$ -androstane and analysed with an Agilent 7890 gas chromatograph (GC) equipped with a VF1 column (30 m length  $\times$  0.25 mm i.d., 0.25 µm film thickness) and a flame ionization detector (FID).



**Figure 1.** Sample locations (black dots) along the transect (map source: US National Park Service, Esri, HERE, DeLorme, MapmyIndia, OpenStreetMap contributors and the GIS user community).

The *n*-alkanoic acids were converted to fatty acid methyl esters (FAMES) with MeOH/HCl (95/5; 70 °C, 8 h). The FAMES were recovered by liquid–liquid extraction with hexane and cleaned over silica, AgNO<sub>3</sub> and zeolite columns as described above before quantification with GC-FID. For quantification of the FAMES, 5 $\alpha$ -androstane was again used as an internal standard. Unfortunately, due to some problems during FAME preparation, not all samples were available for methylation (missing samples: BRO, HUB, HUG, HUM, HUR, KOC).

## 2.3 Leaf wax proxies

Total *n*-alkane and *n*-alkanoic acid concentrations ( $c_{\text{tot}}$ ) were calculated as the sum of C<sub>25</sub> to C<sub>35</sub> and C<sub>20</sub> to C<sub>34</sub> (odd as well as even ones), respectively, and given in µg g<sup>-1</sup> dry weight (dw).

Changes in the average chain length (ACL) of *n*-alkyl lipids can show changes in the input of vegetation type. The ACL was determined by modifying the equation of Poynter et al. (1989). We used odd chain lengths only for *n*-alkanes (Eq. 1) and even chain lengths for *n*-alkanoic acids (Eq. 2).

$$\text{ACL}(n\text{-alkanes}) = \frac{27 \times n\text{-C}_{27} + 29 \times n\text{-C}_{29} + 31 \times n\text{-C}_{31} + 33 \times n\text{-C}_{33}}{n\text{-C}_{27} + n\text{-C}_{29} + n\text{-C}_{31} + n\text{-C}_{33}} \quad (1)$$

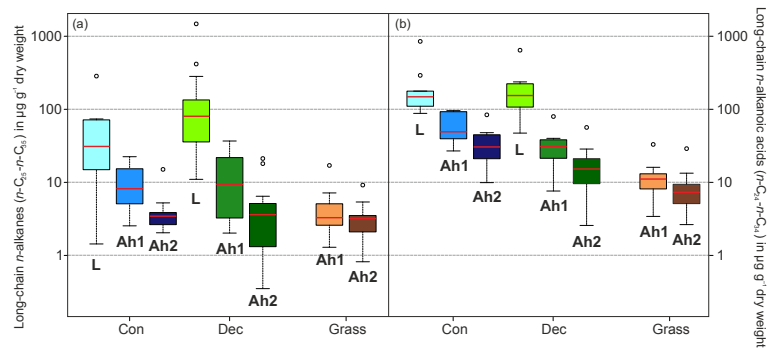


**Figure 2.** Total concentrations of (a) *n*-alkanes and (b) *n*-alkanoic acids in  $\mu\text{g g}^{-1}$  dry weight. Abbreviations: con, coniferous forest sites ( $n = 9$ ); dec, deciduous forest sites ( $n = 14$ ); grass, grassland sites ( $n = 22$ ); L, litter; Ah1, topsoil 1 (0–3 cm); Ah2, topsoil 2 (3–10 cm). Box plots show median (red line), interquartile range (IQR) with upper (75 %) and lower (25 %) quartiles, lowest datum still within  $1.5 \times \text{IQR}$  of lower quartile, and highest datum still within  $1.5 \times \text{IQR}$  of upper quartile. Note that the *y* axis is logarithmic.

$$\text{ACL}(n\text{-alkanoic acids}) = \frac{24 \times n\text{-C}_{24} + 26 \times n\text{-C}_{26} + 28 \times n\text{-C}_{28} + 30 \times n\text{-C}_{30} + 32 \times n\text{-C}_{32}}{n\text{-C}_{24} + n\text{-C}_{26} + n\text{-C}_{28} + n\text{-C}_{30} + n\text{-C}_{32}} \quad (2)$$

The OEP of the *n*-alkanes (Eq. 3) and the EOP of the *n*-alkanoic acids (Eq. 4) can be used as a proxy for degradation and were determined after Hoefs et al. (2002):

$$\text{OEP} = \frac{n\text{-C}_{27} + n\text{-C}_{29} + n\text{-C}_{31} + n\text{-C}_{33}}{n\text{-C}_{26} + n\text{-C}_{28} + n\text{-C}_{30} + n\text{-C}_{32}}, \quad (3)$$

$$\text{EOP} = \frac{n\text{-C}_{24} + n\text{-C}_{26} + n\text{-C}_{28} + n\text{-C}_{30} + n\text{-C}_{32}}{n\text{-C}_{23} + n\text{-C}_{25} + n\text{-C}_{27} + n\text{-C}_{29} + n\text{-C}_{31}}. \quad (4)$$

High OEP values are characteristic of fresh plant material, while the OEP values decrease with ongoing soil organic matter degradation in the topsoil (e.g. Buggle et al., 2010; Zech et al., 2009, 2011b).

#### 2.4 Statistical analysis

First, we tested whether the data were normally distributed (Shapiro and Wilk, 1965) and whether variances of the samples were equal (Levene, 1960). In the case of normality and equal variances, we conducted an analysis of variance (ANOVA) test or otherwise a Kruskal–Wallis test to check for significant differences ( $\alpha = 0.05$ ) between depths horizons within the same vegetation type or between vegetation types within the same horizon, respectively. If the ANOVA/Kruskal–Wallis test indicated significant differences in the means, we applied a “post hoc” test to identify which of the means differ, accounting for the effect of multiple testing. The appropriate post hoc test after ANOVA was selected as recommended by Field (2013): for samples with equal size and equal variance, we applied the Tukey’s honest significance test (Tukey, 1949). In the case of equal variance and unequal sample size, we used the Hochberg test (Hochberg, 1988) and for unequal variances the Games–Howell test (Games and Howell, 1976). After Kruskal–Wallis tests, we performed the non-parametric

Conover–Iman post hoc test with a Bonferroni adjustment of *p* values (Conover and Iman, 1979; Conover, 1999). This test is similar to the well-known Dunn test (Dunn, 1964) but is based on the *t* distribution instead of the *z* distribution. It is statistically more powerful than the Dunn test and better suited for our small sample size.

### 3 Results

#### 3.1 Leaf wax *n*-alkane abundances and chain length patterns

All samples show a dominance of long ( $> \text{C}_{25}$ ) odd-chain *n*-alkanes, characteristic for epicuticular leaf waxes (e.g. Eglinton et al., 1962; Eglinton and Hamilton, 1967; Rieley et al., 1991; Collister et al., 1994). Total *n*-alkane concentrations ( $C_{\text{tot}}$ ) range from 0.4 to  $1468 \mu\text{g g}^{-1}$  dw (Table S3). Such concentrations and huge variability are in agreement with published data from fresh plant material (e.g. Diefendorf et al., 2011; Hoffmann et al., 2013) and from soil and sediments (e.g. Marseille et al., 1999; Freeman and Colarusso, 2001; Liebezeit and Wöstmann, 2009). Differences exist depending on the vegetation type and litter/soil horizon (Fig. 2a) but are mostly not significant (Table S4).

Differences in chain length patterns between deciduous forests, coniferous forests and grasslands are illustrated in Fig. 3 for litter (a), Ah1 (b) and Ah2 (c). The deciduous forest samples are strongly dominated by *n*-C<sub>27</sub>, although its relative abundance decreases from litter to Ah2. However, most of our sampling sites are dominated by beech trees (L11, L13, L14, L16, L17, L18, L20 and L23) that are known to produce mostly *n*-C<sub>27</sub> (Bush and McInerney, 2013, and references therein). To check whether the observed *n*-C<sub>27</sub> dominance could be explained only with the presence of beech we performed the same correlations and plots as mentioned above, excluding the beech-dominated sites. Figure S5 in the Supplement shows that the dominance of *n*-C<sub>27</sub> is less pronounced here and disappears in Ah2. Grass sites are dom-

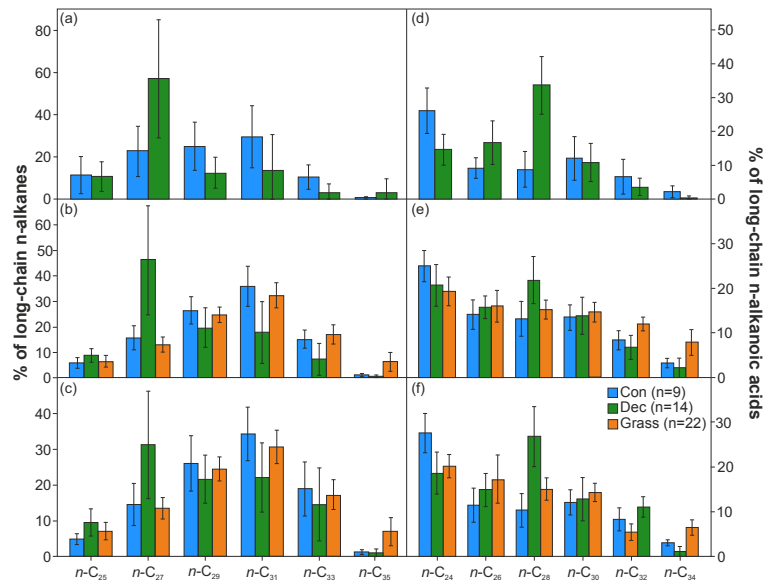


**Figure 3.** Chain length patterns for odd long-chain *n*-alkanes in (a) litter, (b) Ah1 and (c) Ah2, as well as long- and even-chain *n*-alkanoic acids in (d) litter, (e) Ah1 and (f) Ah2.

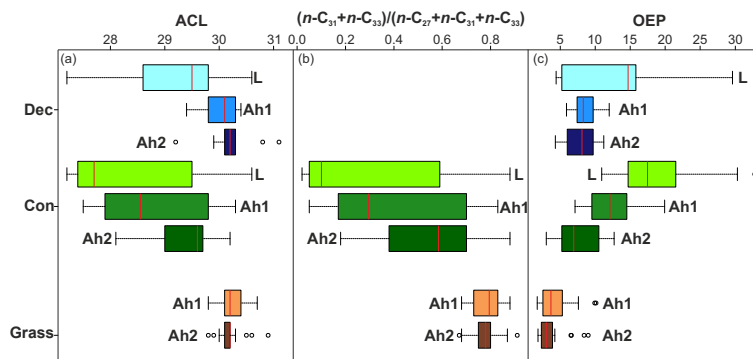


**Figure 4.** Box plots of (a) *n*-alkane ACL, (b)  $(n\text{-}C_{31} + n\text{-}C_{33}) / (n\text{-}C_{27} + n\text{-}C_{31} + n\text{-}C_{33})$  ratio, and (c) OEP. Con: coniferous forest sites ( $n = 9$ ); dec: deciduous forest sites ( $n = 14$ ); grass: grassland sites ( $n = 22$ ); L: litter; Ah1: topsoil 1 (0–3 cm); Ah2: topsoil 2 (3–10 cm). Box plots show median (red line), interquartile range (IQR) with upper (75 %) and lower (25 %) quartiles, lowest datum still within  $1.5 \times$  IQR of lower quartile, and highest datum still within  $1.5 \times$  IQR of upper quartile.

inated by  $n\text{-}C_{31}$  and are also characterized by high abundances of  $n\text{-}C_{33}$  compared to deciduous sites. The con sites show a pattern very similar to that of our grass sites.

The ACLs of the grass and con sites are significantly higher than those of the dec sites (Fig. 4a; grass: Ah1 = 30.5; Ah2 = 30.3; dec: Ah1 = 28.6; Ah2 = 29.6; see Table S6 for  $p$  values). Without the beech-dominated sites, the dec sites' ACL shifts to higher values, but they are still significantly lower than mean ACLs of the grass sites (Fig. S7a). However, significant differences disappear in Ah2 (Table S6). The dec litter samples have lower ACLs (27.5) than the Ah1 (28.6) and Ah2 (29.6). Our grass samples show almost no decrease in ACL from Ah1 (30.5) to Ah2 (30.3), and the con sites likewise show no significant decrease from L to Ah2 (Table S6).

To study past changes in dec vs. grass vegetation, various *n*-alkane ratios have been proposed and used (e.g. Zhang et al., 2006; Lei et al., 2010; Bush and McInerney, 2013; Zech et al., 2013a, b). We tested several *n*-alkane ratios (i.e.  $n\text{-}C_{33} / (n\text{-}C_{27} + n\text{-}C_{33})$ ,  $(n\text{-}C_{31} + n\text{-}C_{33}) / (n\text{-}C_{27} + n\text{-}C_{31} + n\text{-}C_{33})$ , and  $(n\text{-}C_{31} + n\text{-}C_{33}) / (n\text{-}C_{27} + n\text{-}C_{29} + n\text{-}C_{31} + n\text{-}C_{33})$ ) and found the largest differences between grass and dec samples for the ratio  $(n\text{-}C_{31} + n\text{-}C_{33}) / (n\text{-}C_{27} + n\text{-}C_{31} + n\text{-}C_{33})$ . This ratio is low in the dec samples and high in the grass samples (Fig. 4b; dec L: 0.08; Ah1: 0.29; Ah2: 0.56; grass Ah1: 0.79; Ah2: 0.78). Differences between dec and grass are significant in Ah1 and Ah2 (Table S8). Without the beech-dominated sites, the ratio becomes higher for dec but still shows significant differences between dec and grass (Fig. S7b, Table S8).

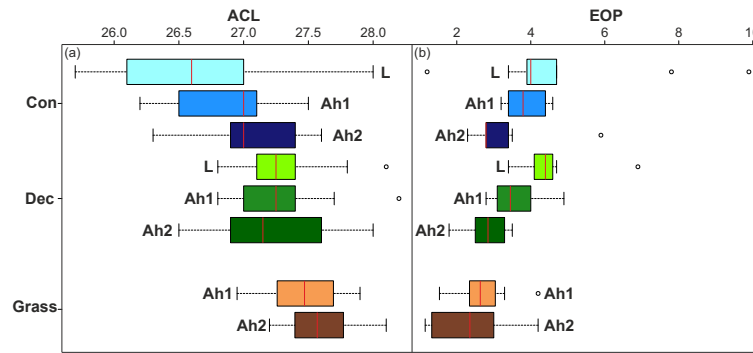


**Figure 5.** Box plots for (a) *n*-alkanoic acid ACL and (b) EOP. Con: coniferous forest sites ( $n = 9$ ); dec: deciduous forest sites ( $n = 14$ ); grass: grassland sites ( $n = 14$ ); L: litter; Ah1: topsoil 1 (0–3 cm); Ah2: topsoil 2 (3–10 cm). Box plots show median (red line), interquartile range (IQR) with upper (75%) and lower (25%) quartiles, lowest datum still within  $1.5 \times$  IQR of lower quartile, and highest datum still within  $1.5 \times$  IQR of upper quartile.

The OEP (or CPI, carbon preference index, which is very similar to the OEP) is often regarded as a proxy for the preservation status of the leaf-wax-derived *n*-alkanes (e.g. Huang et al., 1996; Tipple and Pagani, 2010; Vogts et al., 2012; Wang et al., 2014, and references therein). High OEPs are characteristic of fresh plant material and modern soils (Kirkels et al., 2013; Diefendorf et al., 2011; Collister et al., 1994), whereas low OEPs indicate degradation of *n*-alkanes during pedogenesis and early diagenesis (Marseille et al., 1999; Freeman and Colarusso, 2001; Buggle et al., 2010; Zech et al., 2011a; Wang et al., 2014). OEPs in the samples range from 3 to 32.8, typical for fresh plant material and soils (Table S3). Values significantly decrease from litter (18.4) to Ah1 (12.1) and Ah2 (6.8) for the dec sites, and a minor decrease can be observed in the grass sites (Fig. 4c, Table S9). Significant differences occur between dec and grass sites in all horizons (Table S9).

### 3.2 Leaf wax *n*-alkanoic acid abundances and chain length patterns

All samples show high abundances of long ( $> C_{20}$ ) even-chain *n*-alkanoic acids (Table S10), characteristic of epicuticular leaf waxes (Eglinton and Hamilton, 1967). Many samples also have large amounts of  $C_{16}$  and  $C_{18}$ , yet those are ubiquitous and cannot be considered as leaf wax biomarkers. Total *n*-alkanoic acid concentrations ( $c_{\text{tot}}$  refers here to the sum of  $C_{20}$  to  $C_{34}$ ) range from 3 to  $854 \mu\text{g g}^{-1}$  dw, consistent with previous studies (e.g. Marseille et al., 1999; Jandl et al., 2002). As for the *n*-alkanes, total *n*-alkanoic acid concentrations vary between the vegetation types and horizons (Fig. 2b). In general,  $c_{\text{tot}}$  decreases from litter to Ah1 and Ah2. In contrast to the *n*-alkanes, the highest *n*-alkanoic acid concentrations occur in our con samples. Decrease from litter to Ah1 and Ah2 are only significant in the dec samples (Table S11).

The *n*-alkanoic acid chain length patterns show differences between the different vegetation types (Fig. 3d: litter; 3e: Ah1; 3f: Ah2). While the dec samples are dominated by  $n\text{-}C_{28}$ , the con samples show a maximum for the shorter homologue  $n\text{-}C_{24}$  in the litter, Ah1 and Ah2. The grass sites have high abundances of  $n\text{-}C_{24}$  to  $n\text{-}C_{30}$ , but when compared to dec and con, the relative high  $n\text{-}C_{32}$  and  $n\text{-}C_{34}$  abundances are distinct.

Significant differences in the ACL between the three vegetation types exist and reflect the above-mentioned predominance of various homologues (Fig. 5a, Table S12). While the grass sites show a tendency towards higher ACLs, the con sites tend to have the lowest values. Differences stay significant, even in Ah1 and Ah2 (Table S12).

On the basis of the above-mentioned significant differences between the ACL and the three vegetation types we propose the following three indices, referred to as CDG indices (Eqs. 5–7) for coniferous forests (C), deciduous forests (D) and grasslands (G):

$$\text{Index C} = \frac{n\text{-}C_{24}}{n\text{-}C_{24} + n\text{-}C_{28} + n\text{-}C_{32} + n\text{-}C_{34}}, \quad (5)$$

$$\text{Index D} = \frac{n\text{-}C_{28}}{n\text{-}C_{24} + n\text{-}C_{28} + n\text{-}C_{32} + n\text{-}C_{34}}, \quad (6)$$

$$\text{Index G} = \frac{n\text{-}C_{32} + n\text{-}C_{34}}{n\text{-}C_{24} + n\text{-}C_{28} + n\text{-}C_{32} + n\text{-}C_{34}}. \quad (7)$$

Index C ranges from 0.25 to 0.91, with the highest values for the con sites (Fig. 6a), and shows significant differences between our con and dec samples, as well as between the con and grass in all horizons, but not between the dec and grass locations (Table S13). Index D ranges from 0.03 to 0.62 and has highest values for the dec sites (Fig. 6b). It differs significantly between all vegetation types in L, Ah1 and Ah2, except for con and grass sites in Ah2. It also significantly decreases from L to Ah1 and Ah2 in the dec sites (Table S14). Index G ranges from 0.00 to 0.37 and discriminates between forest and grass sites, with systematically higher values for

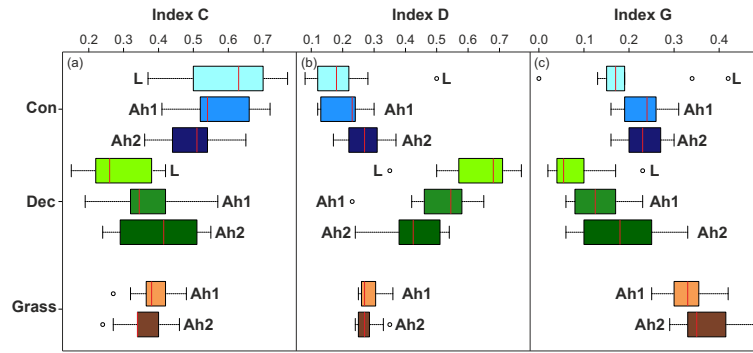


**Figure 6.** Box plots for (a) indices C, (b) D and (c) G. Con: coniferous forest sites ( $n = 9$ ); dec: deciduous forest sites ( $n = 14$ ); grass: grassland sites ( $n = 14$ ); L: litter; Ah1: topsoil 1 (0–3 cm); Ah2: topsoil 2 (3–10 cm). Box plots show median (red line), interquartile range (IQR) with upper (75 %) and lower (25 %) quartiles, lowest datum still within  $1.5 \times$  IQR of lower quartile, and highest datum still within  $1.5 \times$  IQR of upper quartile.

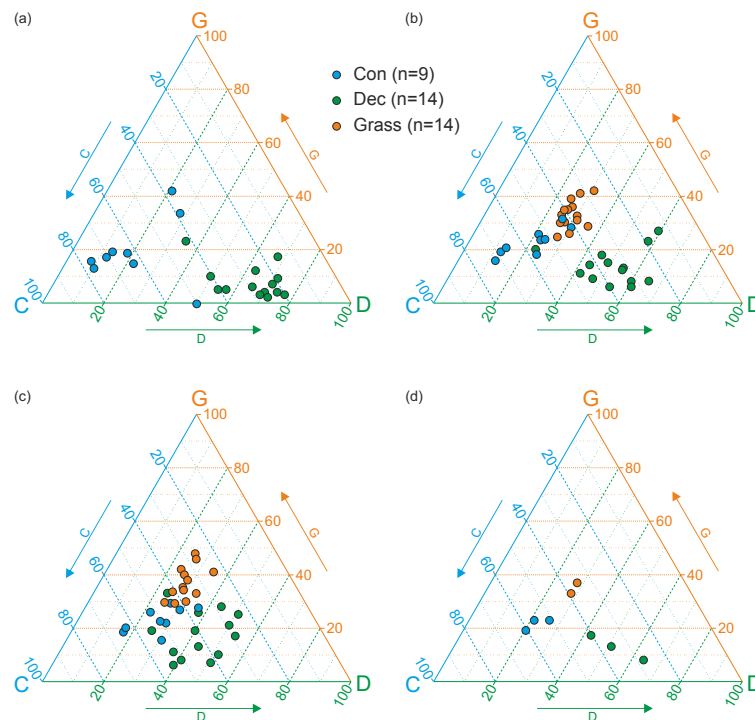


**Figure 7.** Ternary plots for the CDG indices: (a) litter, (b) Ah1 and (c) Ah2, as well as (d) means for vegetation types. Each point represents the mean of litter, Ah1 and Ah2, with regard to con, dec and grass.

the grass sites (Fig. 6c). Like index D, index G shows significant differences between all three vegetation types in all horizons, except for the con and dec locations in Ah1. The index likewise shows a significant decrease from L to Ah2 in the dec samples (Table S15). The CDG indices can conveniently be plotted in ternary diagrams, which illustrate the clusters for the different vegetation types and the scatter within the cluster (Fig. 7).

EOPs in our samples range from 1.2 to 9.9 (Table S16), typical for *n*-alkanoic acids that originate from epicuticular leaf waxes and are found in soils (Killops and Killops, 2005). The EOP decreases significantly from litter to Ah1 and Ah2 in the dec samples (L: 4.3; Ah1: 3.46; Ah2: 2.85; Fig. 5b, Table S16), and without significance in the con samples (L: 4.0; Ah1: 3.8; Ah2: 2.81).

## 4 Discussion

### 4.1 *n*-alkane pattern in litter and topsoil

The lower  $c_{\text{tot}}$  values of the con litter samples compared to the dec litter (median con:  $30.9 \mu\text{g g}^{-1} \text{dw}$ ; dec:  $80.4 \mu\text{g g}^{-1} \text{dw}$ ) are in good agreement with findings of much lower *n*-alkane abundances in conifer needles than deciduous leaves (e.g. Sachse et al., 2006; Zech et al., 2009; Diefendorf et al., 2011; Norris et al., 2013; Tarasov et al., 2013) and in forest soils below conifers (e.g. Almendros et al., 1996). Given these low reported *n*-alkane concentrations in conifer needles, we ascribe the *n*-alkane patterns in the con litter and topsoil samples to the *n*-alkane input from the understorey, and we focus in the following discussion on the differences between grass and dec sites. Our grass soils have very low *n*-alkane abundances (median Ah1,  $3.5 \mu\text{g g}^{-1} \text{dw}$ ), which we interpret to be an artefact of (former) plowing and admixture with inorganic soil material. Based on the data we therefore cannot infer a low *n*-alkane production in grass sites.

#### 4.1.1 *n*-alkanes to distinguish between vegetation types

The domination of *n*-C<sub>27</sub> in our dec samples in all horizons, and the relatively high concentration of *n*-C<sub>31</sub> and *n*-C<sub>33</sub> in the grass samples, implies that the established source-specific compounds, at least along the transect, allow for conclusions to be made regarding the vegetation type that generated them. However, Fig. S5 proves that the pattern is less specific when the beech-dominated sites are excluded. This supports former results and shows that *n*-C<sub>27</sub> is strongly produced by beech trees (Bush and McInerney, 2013, and references therein). The ACL and our proposed *n*-alkane ratio of  $(n\text{-C}_{31} + n\text{-C}_{33}) / (n\text{-C}_{27} + n\text{-C}_{31} + n\text{-C}_{33})$  show significant differences between the dec and the grass sites in Ah1 and Ah2, even when the beech-dominated sites are excluded (Tables S6 and S8). Although *n*-C<sub>27</sub> is not the dominant long odd-chain *n*-alkane in Ah2 at the dec locations that are not dominated by beeches, its percentage in the dec samples is still higher than at the grass sites (Fig. S5), whereas the percentage of *n*-C<sub>31</sub> and *n*-C<sub>33</sub> is the highest in the grass sites in Ah1 as well as in Ah2. Therefore, our results corroborate, at least for the studied transect, that the ACL and our proposed *n*-alkane ratio of  $(n\text{-C}_{31} + n\text{-C}_{33}) / (n\text{-C}_{27} + n\text{-C}_{31} + n\text{-C}_{33})$  allow for differentiation between the input of dec and grass vegetation. Care has to be taken when interpreting palaeovegetation changes solely on the dominance of one *n*-alkane compound over the others (e.g. proxies like  $C_{\text{max}}$ ; Wiesenberg et al., 2015), because this might lead to an underestimation of the deciduous tree input, at least when beech trees were not the main contributors to the soil. Nevertheless, we strongly emphasize that the observed patterns are very likely a regional phenomenon and our results should not be transmitted to other regions with different climate and vegetation types, because *n*-alkane patterns do not work on a

global scale (Bush and McInerney, 2013). Thus, our results underline the need for regional calibrations for the *n*-alkane pattern, because they corroborate its potential for palaeovegetation reconstruction on a regional base.

Although significant differences occur between the dec and grass sites OEP in Ah1 and Ah2, we would not recommend using the OEP as a proxy to distinguish between the two vegetation types, because it can very likely show significant decreases with increasing soil depth, as it does in the dec samples (Table S9), so it is probably strongly influenced by degradation and microbial reworking.

#### 4.1.2 Influence of soil depth on the *n*-alkane pattern

Although we observed no significant decreases in  $C_{\text{tot}}$  from L to Ah1 and Ah2 for the dec and con sites, as well as from Ah1 to Ah2 for all three vegetation forms (Table S4), the slightly decreasing trends in Fig. 2a are most likely due to lipid degradation and admixture with inorganic soil material.

As stated above, the significant decrease in OEP from L to Ah2 in the dec samples (Fig. 4c, Table S9) is probably due to degradation effects. Therefore, despite the wide range of OEPs in modern plants (Bush and McInerney, 2013, and references therein), the OEP can serve as a degradation proxy along our transect. The OEPs in the grass samples show no significant decrease from Ah1 (7.2) to Ah2 (6.5), but the degradation effects here are probably biased by plowing and mixing of Ah1 and Ah2.

The decrease in the relative percentage of the dominant *n*-alkane(s) in the dec and grass samples from L to Ah1 and from Ah1 to Ah2 (Fig. 3a–c) as well as the significant increase in ACL from L to Ah2 in the dec samples (Fig. 4a, Table S6) is probably another indication of the effect of degradation on the *n*-alkane pattern. Our grass samples show an insignificant but decreasing trend in ACL from Ah1 (30.5) to Ah2 (30.3). These observed changes are consistent with the notion that the more abundant homologues are preferentially degraded and lost during pedogenesis. This affects *n*-alkane patterns in soils and sediments (Zech et al., 2009, 2013a, b). Degradation also affects our  $(n\text{-C}_{31} + n\text{-C}_{33}) / (n\text{-C}_{27} + n\text{-C}_{31} + n\text{-C}_{33})$  ratio, which is expressed in the significant increases in the dec samples from litter (0.08) to Ah1 (0.3) to Ah2 (0.56) and in the slightly decreasing trend in the grass samples from 0.84 to 0.80 (Fig. 4b, Table S8).

In order to illustrate and correct for degradation effects, Zech et al. (2009) proposed an endmember model, which was later modified by Zech et al. (2013a, b). We added the dec and grass samples to the dataset for Europe, provided by Zech et al. (2013b). Figure 8 shows the new endmember plot and illustrates that our *n*-alkane ratio differs between grass and dec samples and that it changes depending on the OEP, i.e. with degradation. As already described above, the *n*-alkane ratio is wider for grass samples and lower values are more typical for dec. With increasing degradation, differences seem to become less: the trend lines, or “degradation lines”, for

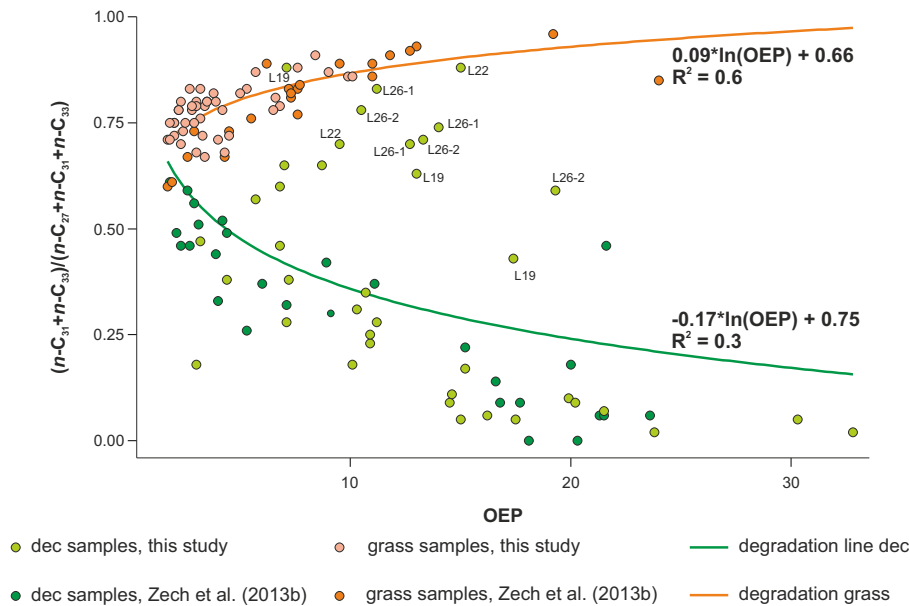


**Figure 8.** Endmember plot modified after Zech et al. (2013b). Degradation lines refer to the complete dataset. Samples that deviated markedly from the degradation lines are labelled and discussed in the text.

grass and dec converge. In principle, the endmember model allows for degradation effects to be tentatively corrected for and for the contribution of grasses versus deciduous trees in (palaeo)samples to be quantified: the equations in Fig. 8 are used to calculate the grass and tree endmember for a specific OEP, and following the rule of proportion % grass can then be estimated as

$$\% \text{ grass} = \frac{n\text{-alkane ratio}_{\text{sample}} - \text{equation}_{\text{degradation line trees}}}{\text{equation}_{\text{degradation line grass}} - \text{equation}_{\text{degradation line trees}}}. \quad (8)$$

Again, we tested whether the endmember plot can be explained only by the presence of beech by applying the same model and plot without the beech-dominated sites. The dec degradation line shifts upward, closer to the grass degradation line (Fig. S17), and  $R^2$  drops from 0.3 to only 0.1, but it still shows a separation of the dec samples from the grass samples. Four sites plot particularly high above the dec degradation line and deserve a closer look. Sample location L19 is a birch forest surrounded by fields, and L26-2 dec is an open forest with birch and oak trees, with a larger number of grasses in the understorey. For both sites, the  $n$ -alkane ratios for Ah1 and Ah2 plot much closer to the grass degradation line than the litter samples, and we speculate that both sites may have been grasslands in the past that were only recently reforested. Since turnover times of  $n$ -alkanes are in the order of decades (e.g. Amelung et al., 2008, and references therein; Wiesenbergl et al., 2004) we would expect to see the  $n$ -alkane pattern prior to reforestation in the upper soil. Unfortunately, we do not have information about former land use at the study locations to verify this speculation. The sample locations L22 (acer, elder, ash, poplar) and L26-1

(acer, oak, beech, fir) are characterized by litter samples that plot close to the grass degradation line. We cannot exclude the possibility that these litter samples and sites are affected by  $n$ -alkane input from grasses, but likely the data simply reflect the large species-specific variability in  $n$ -alkane patterns reported repeatedly in the literature (e.g. Diefendorf et al., 2011; Bush and McInerney, 2013).

In summary, our results show that (1)  $n$ -alkane patterns are systematically different between the investigated dec and grass sites, (2) soil depth/degradation affects the homologue patterns, and (3) endmember modelling is a useful tool for palaeovegetation reconstruction along the transect, but one needs to be aware of the uncertainties related mainly to the large species-specific variability in the  $n$ -alkane patterns. However, the fact that coniferous trees produce only a few  $n$ -alkanes makes respective palaeovegetation reconstructions “blind” for coniferous trees.

#### 4.2 $n$ -alkanoic acid pattern in vegetation and topsoil

To the best of our knowledge, this is the first study which systematically investigates long-chain  $n$ -alkanoic acid patterns in litter and topsoil along a transect that encompasses a range of environmental conditions and vegetation types. Since differences in con concentration compared to dec are much more pronounced in the topsoil than in the litter, we infer that better preservation of  $n$ -alkanoic acids in soils under coniferous forests is the reason for the observed differences, and not higher alkanolic acid production by conifers. This is further consistent with studies showing better preservation of alkanolic acids in soils with low pH typical for conifer-

ous forests, while *n*-alkanes are better preserved in soils with a high pH, more typical for deciduous forests (Bull et al., 2000a; Zocatelli et al., 2012). We again attribute the low  $c_{\text{tot}}$  in the grass sites mainly to plowing and admixture with inorganic soil material.

#### 4.2.1 *n*-alkanoic acids to distinguish between vegetation types

The *n*-alkanoic acid distribution in the vegetation types implies that specific compounds can be used to characterize them (Fig. 3d–f). The *n*-C<sub>24</sub> alkanic acid can represent the input of conifers in L, Ah1 and Ah2; *n*-C<sub>28</sub> shows the contribution of deciduous trees in all horizons; and the relative amount of *n*-C<sub>32</sub> and *n*-C<sub>34</sub> can be used to estimate the grass contribution. From that, we suggest the CDG indices. They show strong differences between the three vegetation types (Fig. 6, Tables S13–S15), which are significant in nearly all horizons, apart from index C, which does not allow a distinction between dec and grass sites (Table S13). The ternary plots of the three indices visualize the discrimination potential by showing clusters for the different vegetation types, although we must emphasize that outliers exist (Fig. 7a–c). Index C based on the dominance of the shorter chain *n*-alkanoic acid C<sub>24</sub>, which might be more strongly affected by microbial degradation and reworking compared to the longer-chain counterparts *n*-C<sub>28</sub>, *n*-C<sub>32</sub> and *n*-C<sub>34</sub> that are included in the D and G indices (Sect. 4.2.2). The ACL of the *n*-alkanoic acids, on the other hand, may not be a particularly useful proxy for palaeovegetation because the observed differences are small (although they are significant, Table S12) and mixing a con and grass signal could falsely yield a dec signal.

#### 4.2.2 Influence of soil depth on the *n*-alkanoic acid pattern

The significant decrease in  $C_{\text{tot}}$  of the dec and con samples from L to Ah2 (Table S11) is most likely attributed to enhanced degradation effects on the acids with increasing soil depth.

The preferential loss of *n*-C<sub>28</sub> (*n*-C<sub>24</sub>) in the dec samples (con samples) can be visualized by comparing the homologue patterns of litter, Ah1 and Ah2 (Fig. 3d–f). This degradation effect is not documented in a significant change in the ACL, and only the con sites show a slight but non-significant increasing trend with increasing soil depth (Fig. 5a, Table S12). The degradation effect of a certain homologue on the CDG indices is illustrated in Figs. 6 and 7. Index D, for example, is high for the dec litter samples but significantly decreases from litter to Ah1 and Ah2 (Table S14). The same applies for index C and G with regard to the con and grass samples, respectively, although the changes are not significant. With the preferential loss of the most abundant compound (*n*-C<sub>28</sub> for dec and *n*-C<sub>24</sub> for con), the respective characteristic index decreases; however, the other two indices un-

avoidably increase. This is illustrated by the clusters moving closer together (Fig. 7b–d). Nevertheless, they still allow for discrimination between the three vegetation types as at least index D and G show significant differences between all three vegetation types in all horizons (Tables S14 and S15). All three indices show a significant decrease (index D) or increase (index C and index G) with soil depth in the dec samples, which implies that they are more prone to degradation under the more alkaline deciduous forest soils. The grass samples do not show changes in ACL or in the indices from Ah1 to Ah2, which we again ascribe to plowing.

The significant decrease in EOP from litter to Ah1 and Ah2 in the dec samples (dec litter: 4.3; Ah1: 3.46; Ah2: 2.85; Fig. 5b) resembles the decrease in the OEP for the *n*-alkanes and suggests that the most abundant (even-numbered) compounds are preferentially degraded during pedogenesis. The decrease in EOP in the con samples is not significant, which we again ascribe to a better preservation of *n*-alkanoic acids in the acidic soils under conifers. Nevertheless, Fig. 5b indicates a decreasing trend in the EOP in the con samples from L to Ah2, probably due to slight degradation effects on the acids in the con Ah1 and Ah2 samples. Grass samples do not show a trend in EOP, which is most likely because of the plowing that affected these sites. Like the OEP, the EOP might thus serve as a proxy for degradation.

Although our results demonstrate that the leaf-wax-derived *n*-alkanoic acids in soils under coniferous forests are less prone to degradation compared to soils under deciduous forests, the risk still exists that the leaf wax contribution from coniferous trees to soil and sedimentary archives might be underestimated when the alkanic acid pattern is not corrected for degradation. The same applies for the deciduous forests and probably also for the grass sites.

Overall, our results show that

- i. *n*-alkanoic acid patterns are significantly different between the investigated dec, con and grass sites;
- ii. the specific CDG indices might be valuable proxies for palaeovegetation;
- iii. degradation affects the homologue patterns and CDG indices, at least in the dec samples, so that procedures to correct for degradation need to be developed and tested.

## 5 Conclusions

We have systematically investigated leaf-wax-derived long-chain *n*-alkane and *n*-alkanoic acid patterns in litter and topsoils along a European transect. Our findings are as follows:

1. Both compound classes show distinct differences depending on the type of vegetation. The vegetation signal is not only found in the litter; it can also be preserved to some degree in the topsoil. The grass sites contain more *n*-C<sub>31</sub> and *n*-C<sub>33</sub> alkanes than the dec sites but less

$n$ -C<sub>27</sub>. The ratio  $(n\text{-C}_{31} + n\text{-C}_{33}) / (n\text{-C}_{27} + n\text{-C}_{31} + n\text{-C}_{33})$  seems to be most suitable to distinguish between those two vegetation types in our study area. Litter and soil samples in coniferous forests are probably biased by the understorey, so vegetation reconstructions solely based on the  $n$ -alkane pattern are blind for coniferous trees. Nevertheless, the  $n$ -alkanes show a great potential for palaeovegetation reconstruction along our transect, but the species-specific absolute and relative variability in the homologue abundances need to be taken into account.

We propose three  $n$ -alkanoic acid indices to distinguish contributions from the three investigated vegetation types: index C is the relative abundance of the C<sub>24</sub>  $n$ -alkanoic acid and represents the input of coniferous trees. Index D is the relative abundance of the C<sub>28</sub>  $n$ -alkanoic acid and is particularly high in litter and in topsoil of deciduous forests. The relative abundance of the C<sub>32</sub> and C<sub>34</sub>  $n$ -alkanoic acids is expressed as index G and shows the contribution from grasses and herbs.

- The homologue patterns of leaf waxes change from litter to Ah1 and Ah2. Although we cannot completely rule out effects related to possible land use and vegetation change in the past, the overall consistent trends imply that degradation plays an important role. Degradation not only lowers the OEP and EOP of  $n$ -alkanes and  $n$ -alkanoic acids, respectively, but also reduces the vegetation-specific differences of the homologue patterns. An updated endmember model is suggested to account for degradation effects on  $n$ -alkanes, but similar procedures still need to be developed and tested for the  $n$ -alkanoic acids before their potential for palaeovegetation reconstructions can be fully exploited.

Overall, our findings suggest that combined investigations of  $n$ -alkane and  $n$ -alkanoic acid distributions on a regional scale have great potential for palaeovegetation reconstruction, although degradation effects need to be taken into account. In particular, with regard to the  $n$ -alkanoic acids, more research is needed to gain a better understanding of those effects.

## 6 Data availability

The dataset we used in this paper is accessible via the Supplement. For the endmember model we combined our dataset with the dataset published in Zech et al. (2013b) at doi:10.1016/j.palaeo.2013.07.023.

**The Supplement related to this article is available online at doi:10.5194/soil-2-551-2016-supplement.**

**Acknowledgements.** We thank P. Neitzel, who contributed in large part to the work in the field and in the laboratory at ETH Zurich, and Q. Lejeune for support in the field, as well as C. Magill for scientific discussions. C. Diebold helped with the laboratory work at the University of Bern. We also acknowledge L. Wüthrich and M. Bliedtner for helpful discussions. The research was funded by the Swiss National Science Foundation (PP00P2 150590).

Edited by: R. Zornoza

Reviewed by: two anonymous referees

## References

- Almendros, G., Sanz, J., and Velasco, F.: Signatures of lipid assemblages in soils under continental Mediterranean forests, *Eur. J. Soil Sci.*, 47, 183–196, doi:10.1111/j.1365-2389.1996.tb01389.x, 1996.
- Amelung, W., Brodowski, S., Sandhage-Hofmann, A., and Bol, R.: Combining biomarker with stable isotope analyses for assessing the transformation and turnover of soil organic matter, in: *Advances in Agronomy*, edited by: Sparks, D. L., Elsevier Inc Academic Press, Burlington, 155–250, doi:10.1016/S0065-2113(08)00606-8, 2008.
- Brincat, D., Yamada, K., Ishiwatari, R., Uemura, H. and Naraoka, H.: Molecular-isotopic stratigraphy of long-chain  $n$ -alkanes in Lake Baikal Holocene and glacial age sediments, *Org. Geochem.*, 31, 287–294, doi:10.1016/S0146-6380(99)00164-3, 2000.
- Buggle, B., Wiesenberg, G. L., and Glaser, B.: Is there a possibility to correct fossil  $n$ -alkane data for postsedimentary alteration effects?, *Appl. Geochem.*, 25, 947–957, doi:10.1016/j.apgeochem.2010.04.003, 2010.
- Bull, I. D., v. Bergen, P. F., Nott, C. J., Poulton, P. R., and Evershed, R. P.: Organic geochemical studies of soils from the Rothamsted classical experiments – V. The fate of lipids in different long-term experiments, *Org. Geochem.*, 31, 389–408, doi:10.1016/S0146-6380(00)00008-5, 2000a.
- Bull, I. D., Nott, C. J., van Bergen, P. F., Poulton, P. R., and Evershed, R. P.: Organic geochemical studies of soils from the Rothamsted classical experiments – VI. The occurrence and source of organic acids in an experimental grassland soil, *Soil Biol. Biochem.*, 32, 1367–1376, doi:10.1016/S0038-0717(00)00054-7, 2000b.
- Bush, R. T. and McNerney, F. A.: Influence of temperature and C<sub>4</sub> abundance on  $n$ -alkane chain length distributions across the central USA, *Org. Geochem.*, 79, 65–73, doi:10.1016/j.gca.2013.04.016, 2015.
- Bush, R. T. and McNerney, F. A.: Leaf wax  $n$ -alkane distributions in and across modern plants: Implications for paleoecology and chemotaxonomy, *Geochim. Cosmochim. Ac.*, 117, 161–179, doi:10.1016/j.gca.2013.04.016, 2013.
- Collister, J. W., Rieley, G., Stern, B., Eglinton, G., and Fry, B.: Compound-Specific Delta-C-13 Analyses of Leaf Lipids from Plants with Differing Carbon-Dioxide Metabolisms, *Org. Geochem.*, 21, 619–627, doi:10.1016/0146-6380(94)90008-6, 1994.
- Conover, W. J.: *Practical Nonparametric Statistics*, 3rd Edn., Wiley, Hoboken, NJ, 1999.

- Conover, W. J. and Iman, R. L.: On multiple-comparisons procedures, Technical Report LA-7677-MS, Los Alamos Scientific Laboratory, Los Alamos, 1979.
- Derenne, S. and Largeau, C.: A review of some important families of refractory macromolecules: composition, origin and fate in soils and sediments, *Soil Sci.*, 166, 833–847, 2001.
- Diefendorf, A. F., Freeman, K. H., Wing, S. L., and Graham, H. V.: Production of n-alkyl lipids in living plants and implications for the geologic past, *Geochim. Cosmochim. Ac.*, 75, 7472–7485, doi:10.1016/j.gca.2011.09.028, 2011.
- Duan, Y. and He, J.: Distribution and isotopic composition of n-alkanes from grass, reed and tree leaves along a latitudinal gradient in China, *Geochem. J.*, 45, 199–207, doi:10.2343/geochemj.1.0115, 2011.
- Dunn, O. J.: Multiple comparisons using rank sums, *Technometrics*, 6, 241–252, 1964.
- Eglinton, G. and Hamilton, R. J.: Leaf epicuticular waxes, *Science*, 156, 1322–1335, doi:10.1126/science.156.3780.1322, 1967.
- Eglinton, G., Hamilton, R. J., Raphael, R. A., and Gonzalez, A. G.: Hydrocarbon Constituents of the Wax Coatings of Plant Leaves: A Taxonomic Survey, *Nature*, 193, 739–742, doi:10.1038/193739a0, 1962.
- Eglinton, T. I. and Eglinton, G.: Molecular proxies for paleoclimatology, *Earth Planet. Sc. Lett.*, 275, 1–16, doi:10.1016/j.epsl.2008.07.012, 2008.
- Feakins, S. J., Kirby, M. E., Cheetham, M. I., Ibarra, Y., and Zimmerman, S. R. H.: Fluctuation in leaf wax D/H ratio from a southern California lake records significant variability in isotopes in precipitation during the late Holocene, *Org. Geochem.*, 66, 48–59, doi:10.1016/j.orggeochem.2013.10.015, 2014.
- Field, A. P.: *Discovering statistics using IBM SPSS Statistics*, 4th Edn., Sage publications, London, 2013.
- Freeman, K. H. and Colarusso, L. A.: Molecular and isotopic records of C4 grassland expansion in the late Miocene, *Geochim. Cosmochim. Ac.*, 65, 1439–1454, doi:10.1016/S0016-7037(00)00573-1, 2001.
- Games, P. A. and Howell, J. F.: Pairwise Multiple Multiple Comparison Procedures with Unequal Unequal N's and/or Variances: A Monte Carlo Study, *J. Educ. Stat.*, 1, 113–125, 1976.
- Gocke, M., Kuzjakov, Y., and Wiesenberg, G. B.: Differentiation of plant derived organic matter in soil, loess and rhizoliths based on n-alkane molecular proxies, *Biogeochemistry*, 112, 23–40, doi:10.1007/s10533-011-9659-y, 2013.
- Guo, N., Gao, J., He, Y., Zhang, Z., and Guo, Y.: Variations in leaf epicuticular n-alkanes in some *Broussonetia*, *Ficus* and *Humulus* species, *Biochem. Syst. Ecol.*, 54, 150–156, doi:10.1016/j.bse.2014.02.005, 2014.
- Hochberg, Y.: A sharper Bonferroni procedure for multiple tests of significance, *Biometrika*, 75, 800–803, 1988.
- Hoefs, M. J. L., Rijpstra, W. I. C., and Sinninghe Damsté, J. S.: The influence of oxic degradation on the sedimentary biomarker record I: evidence from Madeira Abyssal plain turbidites, *Geochim. Cosmochim. Ac.*, 66, 2719–2735, doi:10.5194/bg-11-2455-2014, 2002.
- Hoffmann, B., Kahmen, A., Cernusak, L. A., Arndt, S. K., and Sachse, D.: Abundance and distribution of leaf wax n-alkanes in leaves of *Acacia* and *Eucalyptus* trees along a strong humidity gradient in northern Australia, *Org. Geochem.*, 62, 62–67, doi:10.1016/j.orggeochem.2013.07.003, 2013.
- Huang, Y., Bol, R., Harkness, D. D., Ineson, P., and Eglinton, G.: Post-glacial variations in distributions, 13C and 14C contents of aliphatic hydrocarbons and bulk organic matter in three types of British acid upland soils, *Org. Geochem.*, 24, 273–287, doi:10.1016/0146-6380(96)00039-3, 1996.
- Jandl, G., Schulten, H.-R. and Leinweber, P.: Quantification of long-chain fatty acids in dissolved organic matter and soils, *J. Plant Nutr. Soil Sci.*, 165, 133–139, doi:10.1002/1522-2624(200204)165:2<133::AID-JPLN133>3.0.CO;2-T, 2002.
- Jansen, B., Nierop, K. G. J., Hageman, J. A., Cleef, A. M., and Verstraten, J. M.: The straight-chain lipid biomarker composition of plant species responsible for the dominant biomass production along two altitudinal transects in the Ecuadorian Andes, *Org. Geochem.*, 37, 1514–1536, doi:10.1016/j.orggeochem.2006.06.018, 2006.
- Killops, S. and Killops, V.: *Chemical Stratigraphic Concepts and Tools, Introduction to Organic Geochemistry*, 2nd Edn., Blackwell Publishing Ltd., 166–245, 2005.
- Kirkels, F. M., Jansen, B., and Kalbitz, K.: Consistency of plant-specific n-alkane patterns in plaggan ecosystems: A review, *Holocene* 23, 1355–1368, doi:10.1177/0959683613486943, 2013.
- Lei, G., Zhang, H., Chang, F., Pu, Y., Zhu, Y., Yang, M., and Zhang, W.: Biomarkers of modern plants and soils from Xinglong Mountain in the transitional area between the Tibetan and Loess Plateaus, *Quatern. Int.*, 218, 143–150, doi:10.1016/j.quaint.2009.12.009, 2010.
- Levene, H.: Robust tests for equality of variances, in: *Contributions to Probability and Statistics: Essays in Honor of Harold Hotelling*, edited by: Olkin, I., Ghurye, S. G., Hoefding, W., Madow, W. G., and Mann, H. B., Stanford University Press, Stanford, 278–292, 1960.
- Liebezeit, G. and Wöstmann, R.: n-Alkanes as Indicators of Natural and Anthropogenic Organic Matter Sources in the Siak River and its Estuary, E Sumatra, Indonesia, *Bull. Environ. Contam. Toxicol.*, 83, 403–409, doi:10.1007/s00128-009-9734-4, 2009.
- Maffei, M.: Chemotaxonomic significance of leaf wax alkanes in the gramineae, *Biochem. Syst. Ecol.*, 24, 53–64, doi:10.1016/0305-1978(95)00102-6, 1996.
- Maffei, M., Badino, S. and Bossi, S.: Chemotaxonomic significance of leaf wax n-alkanes in the Pinales (Coniferales), *J. Biol. Res.*, 1, 3–19, 2004.
- Marseille, F., Disnar, J. R., Guillet, B., and Noack, Y.: n-Alkanes and free fatty acids in humus and A1 horizons of soils under beech, spruce and grass in the Massif-Central (Mont-Lozère), France, *Eur. J. Soil Sci.*, 50, 433–441, doi:10.1046/j.1365-2389.1999.00243.x, 1999.
- Norris, C. E., Dungait, J. A. J., Joynes, A., and Quideau, S. A.: Biomarkers of novel ecosystem development in boreal forest soils, *Org. Geochem.*, 64, 9–18, doi:10.1016/j.orggeochem.2013.08.014, 2013.
- Nguyen Tu, T. T., Egasse, C., Zeller, B., Bardoux, G., Biron, P., Ponge, J.-F., David, B., and Derenne, S.: Early degradation of plant alkanes in soils: A litterbag experiment using 13C-labelled leaves, *Soil Biol. Biochem.*, 43, 2222–2228, doi:10.1016/j.soilbio.2011.07.009, 2011.

- Otto, A. and Simpson, M.: Degradation and Preservation of Vascular Plant-derived Biomarkers in Grassland and Forest Soils from Western Canada, *Biogeochemistry*, 74, 377–409, doi:10.1007/s10533-004-5834-8, 2005.
- Poynter, J. G., Farrimond, P., Robinson, N., and Eglinton, G.: Aeolian-Derived Higher Plant Lipids in the Marine Sedimentary Record: Links with Palaeoclimate, in: *Paleoclimatology and Paleometeorology: Modern and Past Patterns of Global Atmospheric Transport*, edited by: Leinen, M. and Sarinthein, M., Springer Netherlands, 435–462, 1989.
- Rieley, G., Collier, R. J., Jones, D. M., Eglinton, G., Eakin, P. A., and Fallick, A. E.: Sources of Sedimentary Lipids Deduced from Stable Carbon Isotope Analyses of Individual Compounds, *Nature*, 352, 425–427, doi:10.1038/352425a0, 1991.
- Rommerskirchen, F., Plader, A., Eglinton, G., Chikaraishi, Y., and Rullkötter, J.: Chemotaxonomic significance of distribution and stable carbon isotopic composition of long-chain alkanes and alkan-1-ols in C4 grass waxes, *Org. Geochem.*, 37, 1303–1332, doi:10.1016/j.orggeochem.2005.12.013, 2006.
- Sachse, D., Radke, J., and Gleixner, G.:  $\delta D$  values of individual n-alkanes from terrestrial plants along a climatic gradient – Implications for the sedimentary biomarker record, *Org. Geochem.*, 37, 469–483, doi:10.1016/j.orggeochem.2005.12.003, 2006.
- Schatz, A.-K., Zech, M., Buggle, B., Gulyás, S., Hambach, U., Marković, S. B., Sümege, P., and Scholten, T.: The late Quaternary loess record of Tokaj, Hungary: Reconstructing palaeoenvironment, vegetation and climate using stable C and N isotopes and biomarkers, *Quatern. Int.*, 240, 52–61, doi:10.1016/j.quaint.2010.10.009, 2011.
- Schefuß, E., Ratmeyer, V., Stuu, J.-B. W., Jansen, J. H. F., and Sinninghe Damsté, J. S.: Carbon isotope analyses of n-alkanes in dust from the lower atmosphere over the central eastern Atlantic, *Geochim. Cosmochim. Ac.*, 67, 1757–1767, doi:10.1016/S0016-7037(02)01414-X, 2003.
- Schwark, L., Zink, K., and Lechterbeck, J.: Reconstruction of post-glacial to early Holocene vegetation history in terrestrial Central Europe via cuticular lipid biomarkers and pollen records from lake sediments, *Geology*, 30, 463–466, doi:10.1130/0091-7613(2002)030<0463:ropteh>2.0.co;2, 2002.
- Shapiro, S. S. and Wilk, M. B.: An analysis of variance test for normality (complete samples), *Biometrika*, 52, 591–611, doi:10.1093/biomet/52.3-4.591, 1965.
- Shepherd, T. and Wynne Griffiths, D.: The effects of stress on plant cuticular waxes, *New Phytol.*, 171, 469–499, doi:10.1111/j.1469-8137.2006.01826.x, 2006.
- Tarasov, P. E., Müller, S., Zech, M., Andreeva, D., Diekmann, B., and Leipe, C.: Last glacial vegetation reconstructions in the extreme-continental eastern Asia: Potentials of pollen and n-alkane biomarker analyses, *Quatern. Int.*, 290–291, 253–263, doi:10.1016/j.quaint.2012.04.007, 2013.
- Tipple, B. J. and Pagani, M.: A 35 Myr North American leaf-wax compound-specific carbon and hydrogen isotope record: Implications for C4 grasslands and hydrologic cycle dynamics, *Earth Planet. Sc. Lett.*, 299, 250–262, doi:10.1016/j.epsl.2010.09.006, 2010.
- Tipple, B. J. and Pagani, M.: Environmental control on eastern broadleaf forest species' leaf wax distributions and D/H ratios, *Geochim. Cosmochim. Ac.*, 111, 64–77, doi:10.1016/j.gca.2012.10.042, 2013.
- Tukey, J.: Comparing Individual Means in the Analysis of Variance, *Biometrics*, 5, 99–114, 1949.
- Vogts, A., Schefuß, E., Badewien, T., and Rullkötter, J.: n-Alkane parameters from a deep sea sediment transect off southwest Africa reflect continental vegetation and climate conditions, *Org. Geochem.*, 47, 109–119, doi:10.1016/j.orggeochem.2012.03.011, 2012.
- Vysloužilová, B., Ertlen, D., Šefrna, L., Novak, T., Viragh, K., Rué, M., Campaner, A., Dreslerová, D., and Schwartz, D.: Investigation of vegetation history of buried chernozem soils using near-infrared spectroscopy (NIRS), *Quatern. Int.*, 365, 203–211, doi:10.1016/j.quaint.2014.07.035, 2015.
- Wang, N., Zong, Y., Brodie, C. R., and Zheng, Z.: An examination of the fidelity of n-alkanes as a palaeoclimate proxy from sediments of Palaeolake Tianyang, South China, *Quatern. Int.*, 333, 100–109, doi:10.1016/j.quaint.2014.01.044, 2014.
- Wiesenberg, G. L. B., Schwarzbauer, J., Schmidt, M. W. I., and Schwark, L.: Source and turnover of organic matter in agricultural soils derived from n-alkane/n-carboxylic acid compositions and C-isotope signatures, *Org. Geochem.*, 35, 1371–1393, 2004.
- Wiesenberg, G. L. B., Andreeva, D. B., Chimitdorgieva, G. D., Erbaeva, M. A., and Zech, W.: Reconstruction of environmental changes during the late glacial and Holocene reflected in a soil-sedimentary sequence from the lower Selenga River valley, Lake Baikal region, Siberia, assessed by lipid molecular proxies, *Quatern. Int.*, 365, 190–202, 2015.
- Wöstmann, R.: Biomarker in torfbildenden Pflanzen und ihren Ablagerungen im nordwestdeutschen Küstenraum als Indikatoren nacheiszeitlicher Vegetationsänderungen, Fakultät für Mathematik und Naturwissenschaft, Carl von Ossietzky Universität, Oldenburg, p. 233, 2006.
- Zech, M., Buggle, B., Leiber, K., Markovic, S., Glaser, B., Hambach, U., Huwe, B., Stevens, T., Sümege, P., Wiesenberg, G. and Zöllner, L.: Reconstructing Quaternary vegetation history in the Carpathian Basin, SE Europe, using n-alkane biomarkers as molecular fossils – Problems and possible solutions, potential and limitations, *Quaternary Sci. J.*, 58, 148–155, 2009.
- Zech, M., Andreev, A., Zech, R., Müller, S., Hambach, U., Frechen, M., and Zech, W.: Quaternary vegetation changes derived from a loess-like permafrost palaeosol sequence in northeast Siberia using alkane biomarker and pollen analyses, *Boreas*, 39, 540–550, doi:10.1111/j.1502-3885.2009.00132.x, 2010.
- Zech, M., Zech, R., Buggle, B., and Zöllner, L.: Novel methodological approaches in loess research – interrogating biomarkers and compound-specific stable isotopes, *Eiszeitalter Gegenwart-Quatern. Sci. J.*, 60, 170–187, 2011a.
- Zech, M., Pedentchouk, N., Buggle, B., Leiber, K., Kalbitz, K., Markovic, S., and Glaser, B.: Effect of leaf-litter decomposition and seasonality on D/H isotope ratios of n-alkane biomarkers, *Geochim. Cosmochim. Ac.*, 75, 4917–4928, 2011b.
- Zech, M., Krause, T., Meszner, S. and Faust, D.: Incorrect when uncorrected: Reconstructing vegetation history using n-alkane biomarkers in loess-paleosol sequences – A case study from the Saxonian loess region, Germany, *Quatern. Int.*, 296, 108–116, doi:10.1016/j.quaint.2012.01.023, 2013a.
- Zech, R., Zech, M., Marković, S., Hambach, U., and Huang, Y.: Humid glacial, arid interglacial? Critical thoughts on pedogenesis and paleoclimate based on multi-proxy analyses of the loess-paleosol sequence Crvenka, Northern Serbia, *Palaeogeogr.*

- Palaeocl., 387, 165–175, doi:10.1016/j.palaeo.2013.07.023, 2013b.
- Zhang, Z., Zhao, M., Eglinton, G., Lu, H., and Huang, C.-Y.: Leaf wax lipids as paleovegetational and paleoenvironmental proxies for the Chinese Loess Plateau over the last 170 kyr, *Quaternary Sci. Rev.*, 25, 575–594, doi:10.1016/j.quascirev.2005.03.009, 2006.
- Zocatelli, R., Lavrieux, M., Disnar, J.-R., Le Milbeau, C., Jacob, J., and Bréheret, J.: Free fatty acids in Lake Aydat catchment soils (French Massif Central): sources, distributions and potential use as sediment biomarkers, *J. Soils Sediments*, 12, 734–748, doi:10.1007/s11368-012-0505-1, 2012.